ARTICLE

Altered Acyl Chain Length Specificity of *Rhizopus delemar* Lipase Through Mutagenesis and Molecular Modeling

Robert R. Klein*, Gregory King, Robert A. Moreau, and Michael J. Haas

ERRC, ARS, USDA, Wyndmoor, Pennsylvania 19038

ABSTRACT: The acyl binding site of *Rhizopus delemar* prolipase and mature lipase was altered through site-directed mutagenesis to improve lipase specificity for short- or medium-chain length fatty acids. Computer-generated structural models of *R. delemar* lipase were used in mutant protein design and in the interpretation of the catalytic properties of the resulting recombinant enzymes. Molecular dynamics simulations of the double mutant, val209trp + phe112trp, predicted that the introduction of trp112 and trp209 in the acyl binding groove would sterically hinder the docking of fatty acids longer than butyric acid. Assayed against a mixture of triacylglycerol substrates, the val209trp + phe112trp mature lipase mutant showed an 80-fold increase in the hydrolysis of tributyrin relative to the hydrolysis of tricaprylin while no triolein hydrolysis was detected. By comparison, the val94Trp mutant, predicted to pose steric or geometric constraints for docking fatty acids longer than caprylic acid in the acyl binding groove, resulted in a modest 1.4-fold increase in tricaprylin hydrolysis relative to the hydrolysis of tributyrin. Molecular models of the double mutant phe95asp + phe214arg indicated the creation of a salt bridge between asp95 and arg214 across the distal end of the acyl binding groove. When challenged with a mixture of triacylglycerols, the phe95asp + phe214arg substitutions resulted in an enzyme with 3-fold enhanced relative activity for tricaprylin compared to triolein, suggesting that structural determinants for medium-chain length specificity may reside in the distal end of the acyl binding groove. Attempts to introduce a salt bridge within 8 Å of the active site by the double mutation leu146lys + ser115asp destroyed catalytic activity entirely. Similarly, the substitution of polar Gln at the rim of the acyl binding groove for phe112 largely eliminated catalytic activity of the lipase.
Lipids 32, 123–130 (1997).

Lipases (acylglycerol acylhydrolases, EC 3.1.1.3) are enzymes that catalyze reversibly the cleavage of ester bonds of triacylglycerols to yield free fatty acids, diacylglycerols, and monoacylglycerols. Lipases are unique among the family of serine esterases in that their catalytic activity is greatly enhanced by the presence of a lipid–water interface, a phenomenon known as interfacial activation (1–3). Various lipases show strong regiospecificity and varying degrees of selectivity and stereospecificity toward different fatty acids (4–6). For industrial application, lipases with pronounced specificity (regio-, stereo-, or fatty acid specificity) are of special interest as these specificities may be exploited to produce products not obtainable by conventional chemical catalysts (7,8).

The fungus *Rhizopus delemar* (presently designated *R. oryzae*) produces extracellular lipases, one of which has been extensively characterized. The *R. delemar* lipase (*Rd* lipase) has been purified and characterized (9), a complementary DNA (cDNA) encoding the enzyme cloned and sequenced (10), and the mature (269 amino acids) and proenzyme (includes 97 amino acid propeptide) forms of the lipase expressed to high levels in *Escherichia coli* (11). *Rd* lipase, like the closely related *Rhizomucor miehei* and *Humicola lanuginosa* lipases, is termed a 1,3-specific lipase, as it exhibits strong preference for the hydrolysis of ester bonds at the *sn*-1 and *sn*-3 positions of a triacylglycerol. The crystal structure of *Rd* lipase has been solved at 2.6 Å resolution (12). The molecular architecture of the enzyme comprises a single, roughly spherical domain containing predominantly parallel β-sheets with conserved α-helices packed on either side. The active center consists of a triad of ser145, his257 and asp204, while an oxyanion hole, presumably formed in the active species by the hydroxyl and main-chain amide groups of thr83, is postulated to stabilize the tetrahedral transition state intermediate (12). In *Rd* lipase, as in all lipases studied, the catalytic center is buried beneath a surface loop or lid consisting of a short amphipathic helix (2,12). The acyl binding region of *Rd* lipase consists of a short hydrophobic trough on the enzyme surface beneath the lid. After absorption to the lipid–water interface, the lid helix is displaced. As a result of this conformational change, the active site is exposed, the oxyanion hole is formed and a large hydrophobic surface is created. This conformational change along with the composition of the lipid substrate constitutes the dominant factors in modulating lipase activities at the oil–water interface (2,12,13).

A major objective of protein engineering efforts is to improve the substrate specificity of the enzyme or create novel catalytic activities by site-directed mutagenesis. Engineering the substrate binding region may tailor the lipase to a particu-

*To whom correspondence should be addressed at USDA, ARS, ERRC, 600 E. Mermaid Lane, Wyndmoor, PA 19038.

Abbreviations: cDNA, complementary DNA; IPTG, isopropyl-B-D-thiogalactoside; Phe, phenylalanine; *Rd, Rhizopus delemar*; TB, tributyrin; TC, tricaprylin; TL, trilaurin; TO, triolein; Tris, *tris*(hydroxymethyl)aminomethane; val, valine.

lar substrate, alter enantioselectivity, or even broaden the substrate specificity of the enzyme. Joerger and Haas (14) initiated studies to alter the chain length selectivity of *Rd* lipase through site-directed mutagenesis. The authors utilized the crystal structure of *R. miehei* lipase (15,16) to identify corresponding residues in the substrate binding region of *Rd* lipase to target for mutagenesis. The recent elucidation of the three-dimensional structure of *Rd* lipase determined by X-ray crystallography (12) provided necessary structural information for more precise identification of the molecular determinants of fatty acyl chain specificity of this enzyme. Utilizing computer-aided molecular modeling, we have constructed a series of single and double amino acid substitution mutants in the acyl binding groove of *Rd* lipase in an attempt to identify the molecular determinants of acyl chain length specificity. The effect of amino acid substitutions on catalytic activity and chain length specificity is discussed in relation to the structural effect of the mutation as predicted by computer-aided molecular models.

MATERIALS AND METHODS

Site-directed mutagenesis. To facilitate site-directed mutagenesis, an 1100 bp *Nco*I-*Bam*HI fragment from plasmid pET 11d-1231 (pET11d recombinant plasmid containing *Rd* prolipase open reading frame sequence; Ref. 14) was subcloned into M13BM20RF phage (Boehringer Mannheim Corp., Indianapolis, IN). Site-directed mutants were generated as detailed in the site-directed mutagenesis protocol provided by the supplier (Amersham Corp., Arlington Heights, IL). To construct double mutants, single-strand DNA containing single amino acid substitutions was used as template for an additional cycle of site-directed mutagenesis. Mutated *Nco*I-*Bam*HI fragments were sequenced (17) and cloned into plasmid pET 15b (Novagen Corp., Madison, WI) for synthesis of recombinant prolipase in *E. coli*. To obtain the same mutations in the mature form of the *Rd* lipase, a 600 bp *Kpn*I-*Eco*RI fragment encompassing the mutations in the prolipase gene was subcloned into plasmid pET 11d-f1-431 (pET 11d recombinant plasmid harboring complete *Rd* mature lipase encoding sequence; Ref. 14) in place of wild-type sequences.

Synthesis and purification of recombinant lipases. Escherichia coli BL21(DE3) cells were transformed with recombinant pET-lipase plasmids and grown in liquid culture media (M9ZB + 100 µg/mL carbenicillin) at 37°C as previously described (18). Synthesis of recombinant lipase was induced by the addition of IPTG to a final concentration of 10 µM (culture OD_{600} = 1.0). Cells were harvested 1.5 to 2 h after IPTG addition by centrifugation (5,500 × *g*, 15 min). Cell pellets were resuspended, lysed, and proteinaceous inclusion bodies obtained (11). Proteinaceous inclusion bodies were solubilized with 8 M urea and the enzyme refolded essentially as described (11) except that the refolded lipases were not further purified by affinity chromatography.

Determination of lipase activity. Initial visual screening of lipase activity utilized a rhodamine plate assay (19). BL21(DE3) cells harboring pET-prolipase plasmids were induced with IPTG and collected by centrifugation. Cells were lysed by sonicating in 50 mM Tris (pH 7.5), 2 mM EDTA, 35 µg/mL phenylmethylsulfonyl fluoride, 1.75 µg/mL leupeptin, and 0.7 µg/mL pepstatin at 4°C. Under these conditions, approximately 1 to 5% of the expressed prolipase was soluble and catalytically active (11,14). Aliquots of *E. coli* lysates containing recombinant prolipases were spotted on media containing a triacylglycerol and rhodamine B. Lipase activity was visualized under ultraviolet light.

Quantitative determination of lipase hydrolytic activity using single triacylglycerol substrates was determined titrimetrically using a VIT 90 Video Titrator (Radiometer, Copenhagen, Denmark). Standard emulsions contained 200 mM olive oil, tricaprylin or tributyrin, 15 mM $CaCl_2$, and 4.2% (wt/vol) gum arabic. Reactions were conducted at 26°C with a set point pH of 7.5. Lipase activity was calculated from the maximum rate of titrant addition using a lipase titrimetric program (20). Titrimetric assays were run in duplicate or triplicate.

Competitive hydrolysis of triacylglycerols was examined in a reaction media containing 100 mM Tris (pH 7.5), 15 mM $CaCl_2$, and equiweight mixtures of tributyrin, tricaprylin, and triolein (2.0% wt/vol). Triacylglycerol mixtures were sonicated and reactions initiated by the addition of lipase (5–10 µg/mL reaction volume). After 30 min (28°C, 250 rpm), reactions were quenched on ice and 5 mg stearyl alcohol (in 100% ethanol) added as an internal standard. Reaction mixtures were extracted with 5 vol hexane for 2 h (250 rpm). Five to 10 µL of the hexane phase were injected into a Hewlett-Packard (Avondale, PA) high-performance liquid chromatograph model 1050 ternary gradient system equipped with an Alltech-Varex Mark III evaporative light-scattering detector (Deerfield, IL) and a 3 × 100 mm LiChrosorb DIOL column (5 µm inner diameter; Chrompack, Inc., Raritan, NJ). The solvents were: A, hexane/acetic acid (1000:1, vol/vol); and B, hexane/isopropanol (100:1, vol/vol). The linear gradient timetable was: 0 min, 100:0; 8 min, 100:0; 10 min, 75:25; 40 min, 75:25; 41 min, 100:0; 60 min 100:0 (% solvent A/% solvent B). Peaks in the chromatograms were identified by comparing retention times to those of triacylglycerol standards. Standard curves were generated for tributyrin, tricaprylin, and triolein based on the injection of seven different amounts of a standard mixture of triacylglycerols. Lipolytic activities were determined by quantifying the disappearance of triacylglycerol substrates compared to control reactions with boiled lipase.

Molecular modeling. All molecular modeling work was conducted using the SYBYL (version 6.0) software package (Tripos Associates, St. Louis, MO) on a SGI Indigo2 workstation (Silicon Graphics, Mountain View, CA). Tripos forcefield parameters were used for all molecular mechanics and molecular dynamics simulations. Nonbonded interaction cutoff of 8 Å was used as was a distance-dependent dielectric constant for electrostatic interactions. All essential protein hydrogens were included in the molecular models. Kollman

United-atoms charges were assigned to all protein atoms while Gasteiger-Huckel charges were assigned to all nonprotein (e.g., lipid) atoms. Energy minimizations were performed with the Powell algorithm, using a change in the rms gradient of less than 0.05 kcal/mol/Å as the convergence criterion. The coordinates of *Rd* lipase were obtained from Z. Derewenda (University of Virginia, Charlottesville, VA). The crystal structure of *Rd* lipase consists of two molecules of the enzyme: one in the closed lid conformation and the second in a conformation intermediate between the closed and open state (12). The coordinates of the enzyme molecule with the partially open lid were used for molecular modeling and substrate docking. The lid was rearranged to a completely open conformation by using the interatomic distances between the α carbons of the lid region of *R. miehei* (Brookhaven Protein DataBase, file 4TGL) (15,16) as constraints in the *Rd* lipase in conjunction with force constants of 50 kcal/mol/Å^2. The structure was subsequently refined *via* energy minimization and molecular dynamics simulations carried out in vacuum at 50 K (total simulation time of 10 ps) followed by a final energy minimization.

To obtain molecular models of mutant *Rd* lipases, the selected amino acid residues were replaced with mutant residues. The optimal conformations of the side chains of mutated residues were obtained by performing systematic grid searches of the relevant torsional angles (at 30° increments). The relevant torsion angles explored included C_α-C_β bonds, C_β-C_α bonds (etc.) as appropriate for the particular substituted amino acid side chain. The lowest energy conformations found in these searches were then refined *via* energy minimization and molecular dynamics simulations. Molecular dynamics simulations were carried out in vacuum at 50 K (total simulation time of 10 ps) followed by a final energy minimization. These structures were utilized as initial enzyme models for docking triacylglycerol substrates.

Models of the triacylglycerol substrates were constructed and energy minimized with the SYBYL version 6.0 software. Initial models of lipase–substrate transition states were obtained by manually positioning the *sn*-3 acyl side chain in the acyl binding groove as defined by transition state analogs (15,21). To build a tetrahedral covalent lipase–substrate complex, the carbonyl carbon of the substrate was converted from its sp^2 configuration to an sp^3-hybridized carbon atom. The conversion of the carbonyl carbon to an sp^3-hybridized carbon atom was necessary to create the correct tetrahedral geometry present in the acyl–enzyme transition state intermediate. The position of the carbonyl carbon of the substrate was adjusted manually to permit hydrogen bonds between the protonated his257, the Oγ of the ser145 hydroxyl group and the oxygen leaving group of the substrate. Furthermore, the distances between the oxyanion of the transition state and the hydroxyl group and main chain amide of thr83 (which comprises the oxyanion hole) were constrained. These bond distances were constrained during the docking procedure and subsequent energy minimization and molecular dynamics simulations. Energy minima of the lipase–substrate complex were found by molecular dynamics simulations in vacuum at 50 K (total simulation time of 10 ps). Molecular dynamics simulations were conducted at low temperature (50 K) to prevent corruption of the conformation of the peptide backbone. Following molecular dynamics simulation, the conformations were subjected to a final energy minimization.

Miscellaneous. Protein concentrations were determined using the bicinchoninic acid protein assay method (Pierce Laboratories, Rockford, IL) using bovine-γ-globulin as protein standard. SDS–12.5% polyacrylamide gel electrophoresis (PAGE) was performed and protein bands on gels were visualized by silver staining (22). Estimates of the relative intensities of protein bands were obtained by video densitometry and analysis of the digitized profile with ImageQuaNT 4.2 software (Molecular Dynamics, Sunnyvale, CA).

RESULTS AND DISCUSSION

Joerger and Haas (14) initiated efforts to alter the acyl chain length specificity of *Rd* lipase through site-directed mutagenesis. Lacking a crystal structure of *Rd* lipase, conserved amino acid residues shown to form the acyl binding groove of *R. miehei* were targeted for mutagenesis in *Rd* lipase. In the present study, we extended the previous mutagenic study aided by the recent elucidation of the crystal structure of *Rd* lipase (Fig. 1). Single and double amino acid substitutions were engineered at discrete positions in the acyl binding groove based largely on structural predictions resulting from molecular dynamics simulations (Fig. 2). Several strategies for altering *Rd* lipase chain length specificity through rational mutagenesis were examined including: introduction of bulky hydrophobic trp residues at discrete positions in the acyl binding groove; creating salt bridges (ionic pairs) across the acyl binding groove by substituting polar or charged residues in the acyl binding groove; and substituting polar amino acids for hydrophobic residues in the acyl binding groove. An additional strategy involved combining selected point mutations of Joerger and Haas (14) into one mutant lipase in an attempt to develop an enzyme with greater substrate specificity.

To engineer a lipase with specificity for short-chain fatty acids, the double mutation F112W + V209W was constructed. Joerger and Haas (14) determined that substitution of trp for phe112 or val209 increased specificity for short-chain (C_4) compared to long-chain fatty acids ($C_{18:1}$). Molecular dynamics simulations of the double mutant V209W + F112W predicted that trp side chains at amino acid positions 112 and 209 of *Rd* lipase would project across the acyl binding groove, thereby posing geometric or steric constraints for the binding of fatty acids longer than butyrate in the acyl groove (Fig. 2A). When screened on rhodamine media containing tributyrin (TB), tricaprylin (TC), trilaurin (TL), or olive oil, hydrolytic activity of the V209W + F112W prolipase was visible only for media containing TB (data not shown). To quantify hydrolytic activity for prolipase and mature lipase mutants, titrimetric assays utilizing single triacylglycerol emulsions were conducted (Figs. 3 and 4). The V209W + F112W mutations resulted in

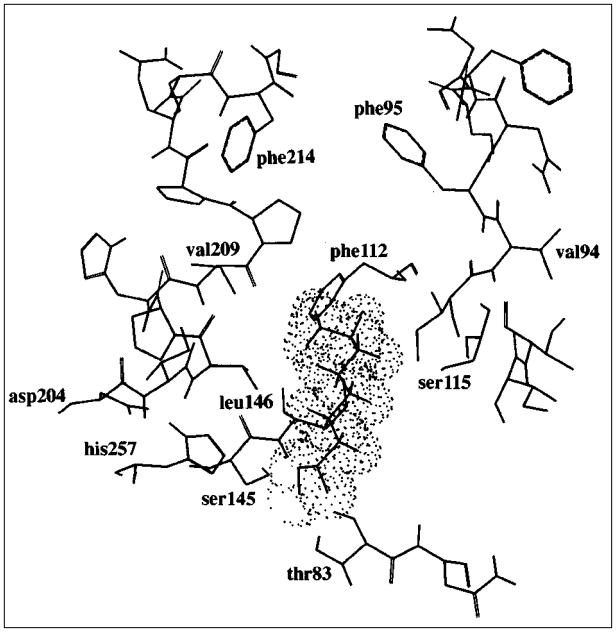

FIG. 1. Structure of the active site region of *Rhizopus delemar* lipase with the *sn*-3 acyl side chain of tricaprylin shown docked into the catalytic center. Only the *sn*-3 acyl side chain of tricaprylin is shown while the remainder of the triacylglyceride is not displayed. The catalytic residues ser, asp, and his are labeled along with thr83 which constitute the oxyanion hole. Selected residues lining the acyl binding and catalytic sites are shown. Sides chains of residues that form part of the acyl binding site targeted for mutagenesis are labeled. The displayed portion of the substrate is depicted with *van der Waals* dots. Models of the docked substrate were calculated by energy minimization and molecular dynamics simulations with bond distance constraints as defined in the Materials and Methods section.

increased specificity for TB though the specific activity of the prolipase and mature lipases for TB was reduced 10- and 1.6-fold, respectively, compared to wild-type enzyme. However, the relative activity of the V209W + F112W mutant toward TB increased substantially since hydrolysis of TC and olive oil was minimal. Relative to wild-type prolipase, the V209W + F112W showed a 9-fold increase in the ratio of TB to olive oil hydrolysis and a 15-fold increase in the ratio of TB to TC hydrolysis. Similarly, the mature lipase V209W + F112W mutant showed an 8.5- and 24-fold increase in the ratio of TB to olive oil and TB to TC hydrolysis, respectively, compared to wild-type lipase.

Quantifying the hydrolytic activities of lipases against single triacylglycerol emulsions provided an initial view of substrate specificity. A more accurate assessment of substrate specificity is obtained by competitive hydrolysis assays utilizing mixed triacylglycerol substrates. In competitive hydrolysis assay conditions, the V209W + F112W prolipase and mature lipase mutants showed strong selectivity for TB. The hydrolytic activity of prolipase V209W + F112W for TB was 10-fold greater than that observed for TC or triolein (TO) (Fig. 5). By comparison, the wild-type prolipase enzyme hydrolyzed TB, TC, and TO to a similar extent in mixed substrate assays. Mature lipase mutant V209W + F112W showed an 80-fold increase in the ratio of TB to TC hydrolysis compared to wild-type lipase while hydrolysis of TO by the V209W + F112W mature lipase was not detected under the present competitive hydrolysis conditions (Fig. 6). The results obtained with either single or mixed triacylglycerol substrates showed that the V209W + F112W double mutant exhibited much stronger selectivity for tributyrin than either of the single amino acid substitutions described by Joerger and Haas (14). The experimental results are in agreement with predictions from molecular dynamics simulations of this double mutant which suggested that the binding of medium- or long-chain length fatty acids may be sterically or geometrically constrained, thereby resulting in a mutant lipase with short-chain fatty acid specificity. It should be noted, however, that the molecular dynamics simulations could not account for the observed reduction in the specific activity of the mutant for tributyrin compared with wild-type enzyme. These observations suggest that the V209W and F112W mutations may have pleiotropic effects on protein structure that remain to be elucidated.

In an attempt to improve the specificity of *Rd* lipase for medium-chain length fatty acids, trp was substituted for V94 in the acyl binding groove. Molecular dynamic simulations predicted that this substitution may pose steric or geometric constraints to the docking of fatty acids longer than caprylate (C_8) in the acyl binding groove (Fig. 2B). The V94W mutation had a modest effect on fatty acid chain length specificity in both the prolipase and mature enzyme. In single substrate hydrolysis assays, a modest 1.6- to 1.8-fold increase in TC hydrolysis relative to TB was observed for V94W enzymes (Figs. 3 and 4). In contrast, the hydrolysis of TC relative to TO by the prolipase and mature enzyme was not altered by the V94W mutation. The results obtained with competitive hydrolysis assays utilizing mixed triacylglycerol substrates paralleled those obtained with single substrate emulsions (Figs. 5 and 6). Compared to wild-type prolipase, the V94W mutant showed a modest 30% reduction in the hydrolysis of TB and TO while the hydrolysis of TC was similar to wild-type levels. The only notable change in hydrolytic activity by introducing this mutation into mature form of *Rd* lipase was a 40% increase in hydrolysis of TC relative to TO. These results indicate that the single substitution of a bulky trp residue at the given location in the acyl binding groove did not markedly alter acyl chain length specificity as predicted by molecular dynamics simulations. The modest increase in specificity for tricaprylin, however, does suggest that a minor molecular determinant of chain length specificity may reside in this position of the acyl binding groove. Hence, it may be feasible to engineer an enzyme with much greater specificity for medium chain length fatty acids by combining the V94W mutation with mutations in other regions of the acyl binding groove shown to impact substrate specificity.

An approach to modify lipase substrate specificity is to alter the structure of the acyl binding groove by creating a salt bridge at discrete positions in the groove. The creation of a salt bridge may alter the conformation of the acyl groove,

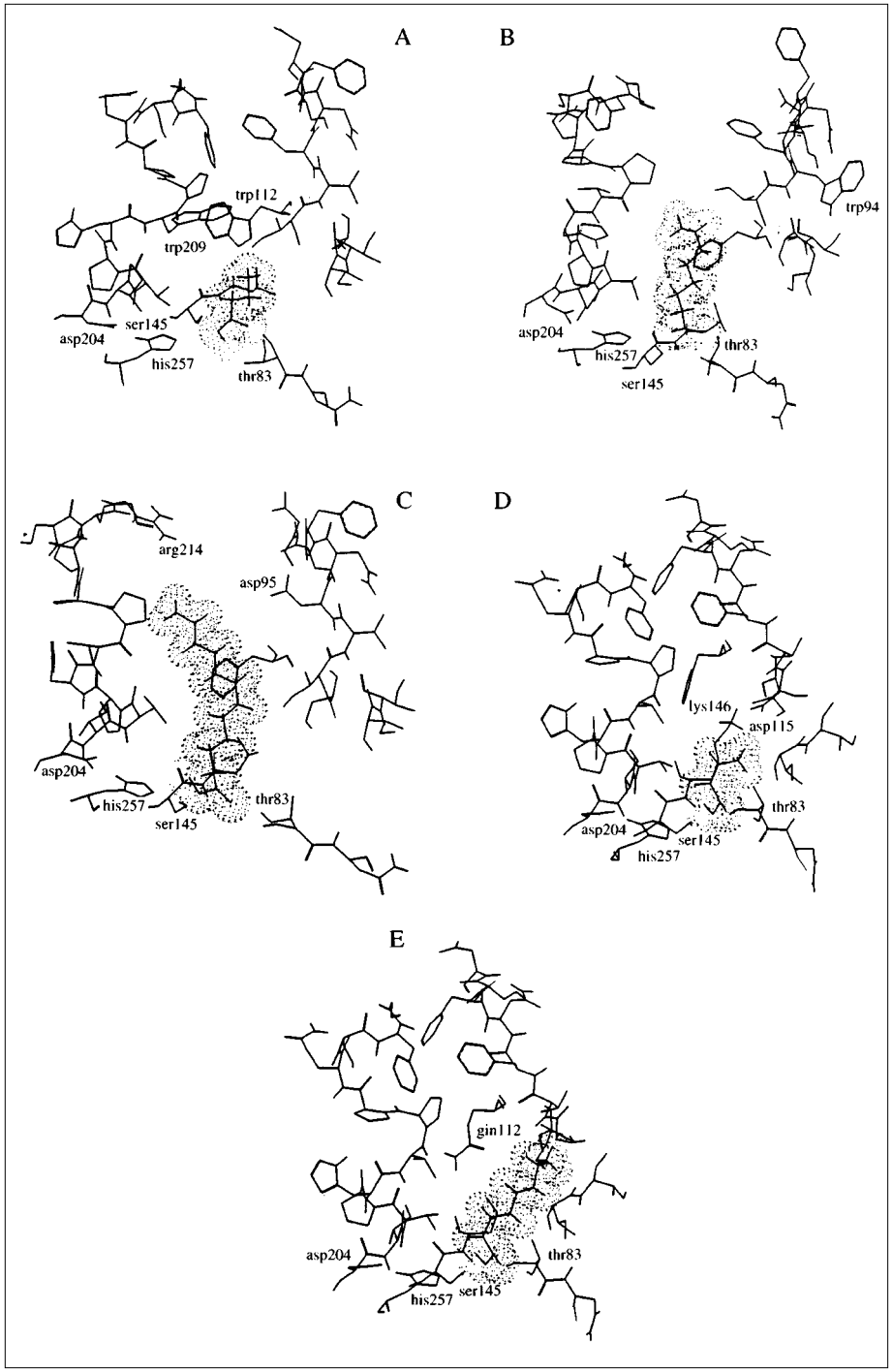

FIG. 2. Models of the active site region of mutated *Rhizopus delemar* lipase with the *sn*-3 acyl side chain of triacylglycerol substrates shown docked in the catalytic center. Only the *sn*-3 acyl side chain of each triacylglycerol is shown while the remainder of the lipid is not displayed. (A) F112W + V209W mutant with docked tributyrin (TB); (B) V94W mutant with docked tricaprylin (TC); (C) F95D + F214R with docked trilaurin (TL); (D) S115D + L146K mutant with docked TB; and (E) F112Q with docked TC. Models of the docked substrates were calculated by energy minimization and molecular dynamics simulations.

thereby constraining or enhancing the binding of select fatty acids. In an attempt to increase selectivity for medium chain length fatty acids, the double mutant F214R + F95D was engineered to position a salt bridge across the distal end of the acyl binding groove (Fig. 2C). In single substrate assays, the prolipase F214R + F95D mutant showed only a slight increase in preference for TC compared to wild-type prolipase (Fig. 3). By comparison, the mature lipase F214R + F95D

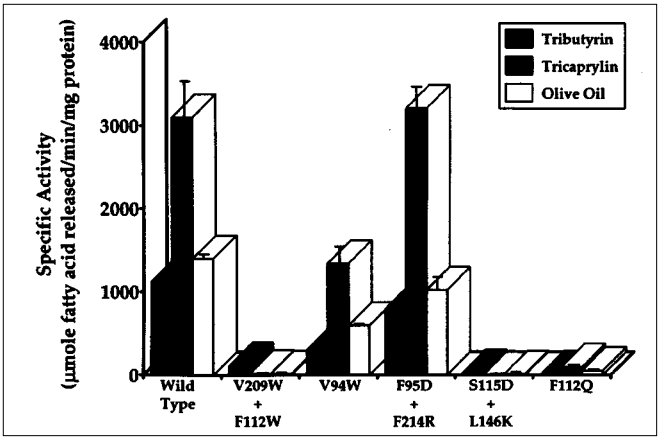

FIG. 3. Comparison between the specific activities of mutant and wild-type *Rhizopus delemar* prolipase using single triacylglycerol substrates. Specific activities were measured titrimetrically against single triacylglycerol emulsions of tributyrin, tricaprylin, or olive oil. Each specific activity is the mean of two or three independent assays.

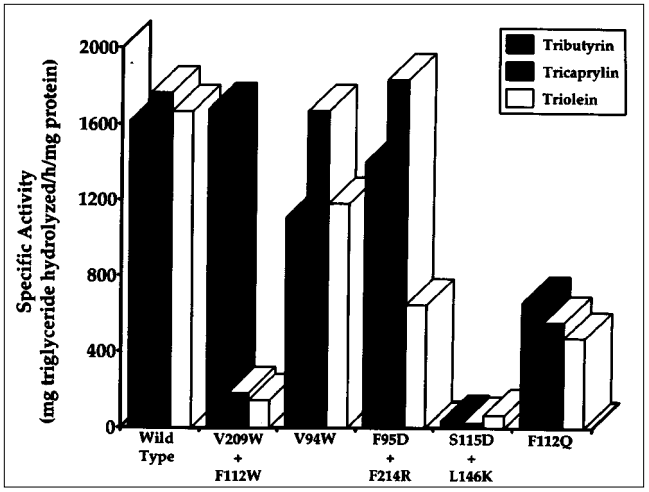

FIG. 5. Comparison between the specific activities of mutant and wild-type *Rhizopus delemar* prolipase using mixed triacylglycerol substrates. Hydrolytic activities were determined by quantifying the amounts of unhydrolyzed triacylglycerols remaining after prolipase incubation with an equiweight mixture of tributyrin, tricaprylin, and triolein. The amount of each triacylglycerol remaining after 30-min incubation with prolipase was determined by HPLC. Competitive hydrolysis assays were conducted a minimum of four times for each enzyme and a representative data set is shown.

mutation showed a 3.3-fold increase in the specific activity toward TC compared to wild-type lipase (Fig. 4). The increased specific activity of the F214R + F95D mature lipase for TC resulted in a 2-fold increase in the relative activity toward TC compared with either TB or olive oil. In competitive hydrolysis assays with triacylglycerol mixtures, the prolipase F214R + F95D mutant exhibited a 2.5-fold increase in the hydrolysis of TC relative to TO while the same mutations in the mature lipase showed a 3.1-fold increase in hydrolysis of TC relative to TO (Figs. 5 and 6). Hence, the introduction of the F95D and F214R mutations increased lipase specificity for medium chain length fatty acids especially for mutations in the mature form of *Rd* lipase. Structurally, whether a salt bridge was actually created between arg214 and asp95 has not been determined although molecular dynamics simulations predicted the ionic pairing of these residues. Nevertheless, it is evident that molecular determinants of acyl chain length specificity reside in this region of the acyl binding site and are amenable to modification.

The double mutation S115D + L146K was engineered to determine the feasibility of introducing charged residues nearer the catalytic center with an objective of impacting acyl chain length specificity (Fig. 2D). Molecular dynamics simulations predicted that the S115D + L146K mutations would create a salt bridge across the acyl binding groove approximately 8 Å from the catalytic center. The position of the salt bridge was predicted to hinder the docking of medium- and

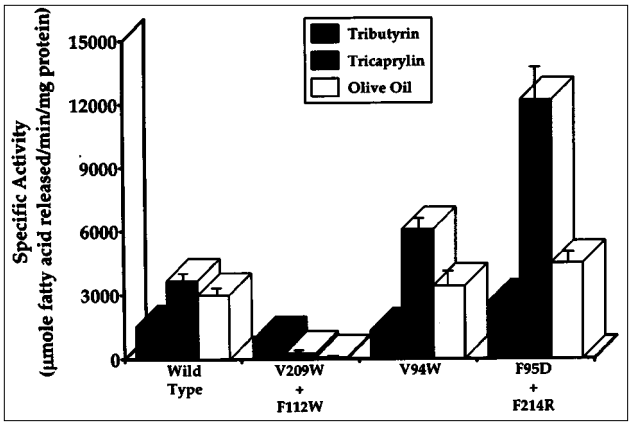

FIG. 4. Comparison between the specific activities of mutant and wild-type mature *Rhizopus delemar* lipase using single triacylglycerol substrates. Specific activities were measured by titrimetric assay against single triacylglycerol emulsions as described for Figure 3.

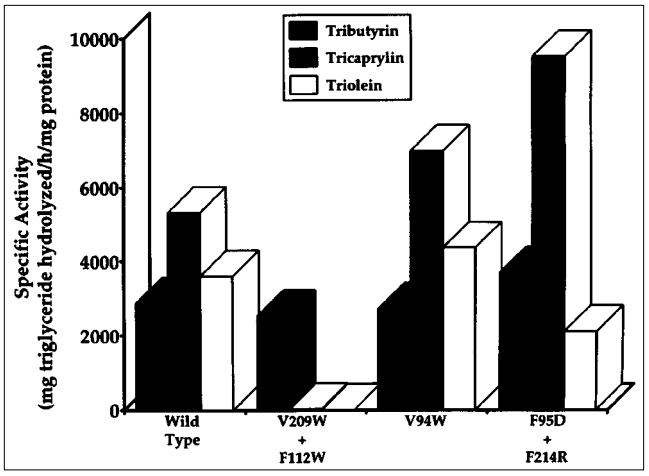

FIG. 6. Comparison between the specific activities of mutant and wild-type *Rhizopus delemar* mature lipase using mixed triacylglycerol substrates. Specific activities of mutant and wild-type mature lipases were determined as described for Figure 5.

long-chain fatty acids and favor the docking of short (C_4) fatty acids in the acyl binding groove. An additional mutation, F112Q, was engineered to determine whether the substitution of a polar residue near the rim of the acyl binding groove would impact acyl chain length specificity (Fig. 2E). The residue phe112 was targeted for mutagenesis since it had been determined that this site is amenable to substitution and molecular dynamics simulations predicted that the docking of long fatty acid chains in the acyl binding groove would be sterically hindered by a polar residue at this position. Hydrolysis assays revealed that the prolipase S115D + L146K mutant was catalytically inactive (Fig. 3). Similarly, introduction of a polar gln for phe112 largely eliminated activity in single substrate emulsions (Fig. 3) and reduced the hydrolytic activity for all three triacylglycerols in mixed emulsions assays (Fig. 5). To determine whether the loss of catalytic activity of the S115D + L146K mutant is due to one or both amino acid substitutions, the single amino acid mutations were examined for catalytic activity. Rhodamine plate and single substrate hydrolysis assays showed that neither the S115D nor the L146K mutants possessed catalytic activity (data not shown). The close proximity of S115 and L146 to the catalytic triad of ser145, his257 and asp204 and the oxyanion hole (thr83) may explain the disruption of catalytic activity. L146 resides within 4 Å of S145 (distance between α carbons). In contrast, F112 is located approximately 12 Å from catalytic ser145 and is located at the rim of the acyl binding groove. Nevertheless, these amino acid substitutions largely eliminated the catalytic activity of the prolipase. The loss of catalytic activity may relate to the disruption of some step in catalysis after the binding of the substrate or to the prevention of efficient penetration of the lipid interface, resulting in lower activity (23). It should be noted that the introduction of polar or charged residues in the acyl binding groove is not necessarily lethal as evidenced by the F95D + F214R mutant and a second double mutant, V206T + F95D, which show strong substrate specificity for medium chain length fatty acids (Klein, R.R., Villeneuve, P., King, G., McNeill, G.P., Moreau, R.A., and Haas, M.J. manuscript in preparation). Hence, our present knowledge of lipase structure–function relationships does not permit an accurate prediction of the lipase phenotype that results from the introduction of charged or polar residues in the acyl binding groove.

In summary, the present study describes attempts toward engineering novel biocatalysts *via* protein engineering of *Rd* lipase. Similar approaches for the rational modification of this lipase are being conducted in other laboratories as well (24). The observed mutant phenotypes indicate that tailoring the substrate specificity of *Rd* lipase is feasible as evidenced by the F112W + V209W and F95D + F214R double mutants. As expected, the major difficulty was predicting the effect of the mutation on catalytic activity. Increasing the likelihood of creating the desired catalytic activity may require mutagenic strategies that simultaneously introduce multiple mutations in a gene (25–27). Computer-aided molecular models may make the process more efficient by identifying critical regions (cassettes) to target for multiple amino acid substitutions, insertions, or deletions. The *Rd* prolipase expression system is well suited for such a mutagenic strategy since a rapid fluorescence visual screen for hydrolytic activity has been developed (14). Unfortunately, the prolipase crystal structure has not been solved, and the presence of the propeptide has significant impact on substrate specificity. Resolution of the crystal structure of the *Rd* prolipase would aid in our understanding of protein structure–function relationship and aid in the tailoring of lipase substrate specificity through protein engineering.

REFERENCES

1. Sarda, L., and Desnuelle, P. (1958) Action of Pancreatic Lipase on Esters in Emulsion, *Biochim. Biophys. Acta 30,* 513–521.
2. Derewenda, Z.S., and Sharp, A.M. (1993) News from the Interface: The Molecular Structures of Triacylglyceride Lipases, *TIBS 18,* 20–25.
3. Derewenda, Z.S. (1995) A Twist in the Tale of Lipolytic Enzymes, *Structural Biology 2,* 347–349.
4. Kazlauskas, R.J. (1994) Elucidating Structure-Mechanism Relationships in Lipases: Prospects for Predicting and Engineering Catalytic Properties, *TIBTECH 12,* 464–472.
5. Cygler, M., Grochulski, P., and Schrag, J.D. (1995) Structural Determinants Defining Common Stereoselectivity of Lipases Toward Secondary Alcohols, *Can. J. Microbiol. 41,* 289–296.
6. Stadler, P., Kovac, A., and Paltauf, F. (1995) Understanding Lipase Action and Selectivity, *Croatica Chemica Acta 68,* 649–674.
7. Quinlan, P., and Moore, S. (1993) Modification of Triglycerides by Lipases: Process Technology and its Application to the Production of Nutritionally Improved Fats, *INFORM 4,* 580–585.
8. Vulfson, E.N. (1994) Industrial Applications of Lipases, in *Lipases, Their Structure, Biochemistry, and Application* (Woolley, P., and Petersen, S.B., eds.) pp. 271–288, Cambridge University Press, Cambridge.
9. Haas, M.J., Cichowicz, D.J., and Bailey, D.G. (1992) Purification and Characterization of an Extracellular Lipase from the Fungus *Rhizopus delemar, Lipids 27,* 571–576.
10. Haas, M.J., Allen, J., and Berka, T.R. (1991) Cloning, Expression and Characterization of a cDNA Encoding a Lipase from *Rhizopus delemar, Gene 109,* 107–113.
11. Joerger, R.D., and Haas, M.J. (1993) Overexpression of a *Rhizopus delemar* Lipase Gene in *Escherichia coli, Lipids 28,* 81–87.
12. Derewenda, U., Swenson, L., Wei, Y., Green, R., Kobos, P.M., Joerger, R., Haas, M.J., and Derewenda, Z.S. (1994) Conformational Lability of Lipases Observed in the Absence of an Oil–Water Interface: Crystallographic Studies of Enzymes from the Fungi *Humicola lanuginosa* and *Rhizopus delemar, J. Lipid Res. 35,* 524–534.
13. Rubin, B. (1994) Grease Pit Chemistry Exposed, *Structural Biology 1,* 568–572.
14. Joerger, R.D., and Haas, M.J. (1994) Alteration of Chain Length Selectivity of a *Rhizopus delemar* Lipase Through Site-Directed Mutagenesis, *Lipids 29,* 377–384.
15. Brzozowski, A.M., Derewenda, U., Derewenda, Z.S., Dodson, G.G., Lawson, D.M., Turkenburg, J.P., Bjorkling, F., Huge-Jensen, B., Patkar, S.A., and Thim, L. (1991) A Model for Interfacial Activation in Lipases from the Structure of a Fungal Lipase–Inhibitor Complex, *Nature 351,* 491–494.
16. Derewenda, Z.S., Derewenda, U., and Dodson, G.G. (1992) The Crystal and Molecular Structure of the *Rhizomucor miehei* Triacylglyceride Lipase at 1.9 Å Resolution, *J. Mol. Biol. 227,* 818–839.

17. Klein, R.R., and Salvucci, M.E. (1992) Photoaffinity Labeling of Mature and Precursor Forms of the Small Subunit of Ribulose-1,5-Bisphosphate Carboxylase/Oxygenase After Expression in *Escherichia coli, Plant Physiol. 98,* 546–553.
18. Sturdier, F.W., Rosenberg, A.H., Dunn, J.J., and Dubendorff, J.W. (1991) Use of T7 RNA Polymerase to Direct the Expression of Cloned Genes. Novagen (Technical Bulletin), Madison WI.
19. Kouker, G., and Jaeger, K.E. (1987) Specific and Sensitive Plate Assay for Bacterial Lipases, *App. Environ. Microbiol. 53,* 211–213.
20. Haas, M.J., Esposito, D., and Cichowicz, D.J. (1995) A Software Package to Streamline the Titrimetric Determination of Lipase Activity, *J. Am. Oil Chem. Soc. 72,* 1405–1406.
21. Uppenberg, J., Öhrner, N., Norin, M., Hult, K., Kleywegt, G.J., Patkar, S., Waagen, V., Anthonsen, T., and Jones, T.A. (1995) Crystallographic and Molecular-Modeling Studies of Lipase B from *Candida antarctica* Reveal a Stereospecificity Pocket for Secondary Alcohols, *Biochemistry 34,* 16838–16851.
22. Morrissey, J.H. (1981) Silver Stain for Proteins in Polyacrylamide Gels: A Modified Procedure with Enhanced Uniform Sensitivity, *Anal. Biochem. 117,* 307–310.
23. Holmquist, M., Clausen, I.G., Patkar, S., Svendsen, A., and Hult, K. (1995) Probing a Functional Role of Glu87 and Trp89 in the Lid of *Humicola lanuginosa* Lipase Through Transesterification Reactions in Organic Solvent, *J. Protein Chem. 14,* 217–224.
24. Schmid, R.D., Menge, U., Schomburg, D., and Spener, F. (1995) Towards Novel Biocatalysts *via* Protein Design: The Case of Lipases, *FEMS Microbiol. Rev. 16,* 253–257.
25. Delagrave, S., Goldman, E.R., and Youvan, D.C. (1993) Recursive Ensemble Mutagenesis, *Protein Eng. 6,* 327–331.
26. Chen, K., and Arnold, F.H. (1993) Tuning the Activity of an Enzyme for Unusual Environments: Sequential Random Mutagenesis of Subtilisin E for Catalysis in Dimethylformamide, *Proc. Natl. Acad. Sci. USA 90,* 5618–5622.
27. Stemmer, W.P.C. (1995) Searching Sequence Space, *Biotechnology 13,* 549–553.

[Received August 26, 1996, and in final revised form December 4, 1996; Revision accepted December 9, 1996]